Some properties of Alfvén waves: Observations in the tail lobes and the plasma sheet boundary layer

A. Keiling,[1] G. K. Parks,[1] J. R. Wygant,[2] J. Dombeck,[2] F. S. Mozer,[1] C. T. Russell,[3] A. V. Streltsov,[4] and W. Lotko[4]

Received 16 November 2004; revised 7 June 2005; accepted 22 June 2005; published 29 October 2005.

[1] We report properties of substorm-related, globally excited Alfvén waves on a temporal scale of 6 to 300 s (3.3 to 167 mHz) at geocentric distances between 5 and 6 R_E. The waves were observed in the tail lobes and the plasma sheet boundary layer (PSBL) by the Polar satellite. In each region we made the following observations: (1) The tail lobe Alfvén waves started at substorm onset as determined from ground magnetometer data. Hence these ULF lobe waves can possibly be used as a new substorm indicator. Although on open field lines, they often showed local standing wave signatures with a large perpendicular scale size and a near-zero net Poynting flux. We do not classify those waves as FLR but interpret them as the superposition of incident and reflected waves. The same oscillations were simultaneously recorded in ground magnetometer data. Immediately poleward of the PSBL, the lobe Alfvén waves traveled earthward (no reflection), suggesting their dissipation in the ionosphere. The lobe waves were superimposed on the signature of a field-aligned current (FAC). The onset of this FAC was simultaneous to the onset of the magnetic substorm bay. (2) The substorm-related PSBL Alfvén waves carried two to three orders of magnitude larger Poynting flux ($\sim$1 erg cm^{-2} s^{-1}) than the lobe Alfvén waves. These PSBL waves were a mixture of standing and traveling Alfvén waves for different frequency ranges. Most Poynting flux was carried in large-scale earthward traveling waves (40–300 s). For one event, we also measured large standing wave components (>0.5 erg cm^{-2} s^{-1}), but such events are rare. In the intermediate range (40–67 s), which overlaps with the Pi2 range, some waves showed clear standing wave signatures. At smaller periods (6–24 s), noninterfering earthward and tailward traveling waves were present with small Poynting fluxes (<0.05 erg cm^{-2} s^{-1}). A trend for increasing E to B ratios with increasing wave frequency was observed. The PSBL waves were left-hand elliptically polarized. The wave vector was within 35° of the background magnetic field direction, suggesting that the waves were phase-mixed. The large-amplitude, substorm-related PSBL Alfvén wave events ($\sim$1 erg cm^{-2} s^{-1}) were found in regions of upward currents.

Citation: Keiling, A., G. K. Parks, J. R. Wygant, J. Dombeck, F. S. Mozer, C. T. Russell, A. V. Streltsov, and W. Lotko (2005), Some properties of Alfvén waves: Observations in the tail lobes and the plasma sheet boundary layer, *J. Geophys. Res.*, *110*, A10S11, doi:10.1029/2004JA010907.

1. Introduction

[2] First predicted by Hannes Alfvén [*Alfvén*, 1942], Alfvén waves have been observed nearly everywhere in the nightside magnetosphere: plasmasphere [*Osaki et al.*, 1998], auroral zone [*Dubinin et al.*, 1990; *Knudsen et al.*, 1992], central plasma sheet (CPS) [*Takahashi et al.*, 1988], plasma sheet boundary layer (PSBL) [*Wygant et al.*, 2000; *Keiling et al.*, 2000], and tail lobes [*Ober et al.*, 2001; *Keiling et al.*, 2001]. Their importance in the substorm process has first been pointed out by *Samson et al.* [1991], who used ground-based observations in the auroral zone and showed that strong ULF (1–10 mHz) Alfvén wave activity was present at both boundaries of the auroral region.

[3] The most energetic Alfvén waves have recently been found in the PSBL. It was shown that these waves are magnetically conjugate to auroras [*Wygant et al.*, 2000; *Keiling et al.*, 2002] and occur during times of substorm expansion phase [*Keiling et al.*, 2000]. Since shear Alfvén waves propagate along magnetic field lines, these observations showed that one important role of these waves is to carry significant electromagnetic energy from remote

[1]Space Sciences Laboratory, University of California, Berkeley, California, USA.
[2]University of Minnesota, Minneapolis, Minnesota, USA.
[3]University of California, Los Angeles, Los Angeles, California, USA.
[4]Dartmouth College, Hanover, New Hampshire, USA.

0148-0227/05/2004JA010907$09.00

regions, possibly the reconnection region, to the auroral regions. Once they reach the auroral region, the Alfvén waves are one candidate for the acceleration of electrons that cause the aurora [*Goertz*, 1984; *Lysak*, 1990; *Chaston et al.*, 2000]. It is suggested that large-scale shear Alfvén waves (presumably those reported in the PSBL) become kinetic Alfvén waves in the small-scale limit, which can provide the parallel electric field necessary for auroral electron acceleration. Some evidence exists that Alfvén waves also accelerate electrons above the auroral acceleration region along magnetic field lines [*Wygant et al.*, 2002; *Morooka et al.*, 2004].

[4] Additional support for their role in auroral phenomena comes from global distribution maps at both low (FAST satellite) and high (Polar satellite) altitude that show that Alfvén waves occur on auroral field lines along the entire auroral oval [*Chaston et al.*, 2003; *Keiling et al.*, 2003].

[5] Thus it has become clear since their prediction about 60 years ago that Alfvén waves are an integral part of substorms. The question of what generates Alfvén waves has been partially answered. There is considerable evidence that compressional MHD waves mode-couple into Alfvén waves, but the mechanism that creates the largest Alfvén waves, those that occur in the PSBL during the substorm expansion phase, is still open to speculation.

[6] The signature of Alfvén waves in the magnetosphere is electric (E) and magnetic (B) field perturbations (both perpendicular to the background magnetic field and to each other) whose ratio equals the local Alfvén speed [*Mallinckrodt and Carlson*, 1978; *Dubinin et al.*, 1990; *Knudsen et al.*, 1992]. In the case of standing Alfvén waves this ratio is modified because of the nodal structure of the E and B fields. If incident and reflected waves are superimposed, the phase relation between E and B is an important property. In the case of standing Alfvén waves, a phase shift of 90° between the two corresponding perpendicular perturbation fields is sufficient evidence for Alfvén waves. Other properties such as polarization, wave frequency, and perpendicular size are also important in determining the wave generation mechanism and how the waves interact with particles.

[7] In this paper we determine properties of standing and traveling Alfvén waves at altitudes above the auroral acceleration region in the tail lobes and the PSBL using data from the Polar spacecraft. We apply spectral analysis to the observed Alfvén waves in the frequency range from 3.3 to 167 mHz (period range: 6 to 300 s) and compare the in situ observations of individual spectral components with ground observations. Ground data is also used to relate the Alfvén waves to substorm onset.

2. Instrumentation

[8] In this study we used Polar spacecraft data from the University of California Berkeley Electric Field Instrument [*Harvey et al.*, 1995], the University of California at Los Angeles Fluxgate Magnetometer [*Russell et al.*, 1995], the University of Iowa Hydra Plasma Instrument [*Scudder et al.*, 1995], and the Ultraviolet Imager of the University of Washington [*Torr et al.*, 1995]. Details of each instrument can be found in the relevant publication.

[9] In addition to Polar data, we utilized magnetometer data from the Canadian Auroral Network for the Open Unified Study (CANOPUS) [*Rostoker et al.*, 1995] and the Geological Survey of Canada.

3. Observations

[10] In this study, we investigated substorm events. Two of these events (9 May 1997 and 23 May 1996) are presented in detail to illustrate our analysis method and to show some properties of Alfvén waves in the tail lobe and the PSBL. Instead of presenting the two events one after the other, this section is organized by topic (sections 3.1 to 3.4) showing both events side-by-side in each subsection. After giving overviews, we will present various results related to FAC and Alfvén wave signatures as recorded on the ground and in space during these two events.

3.1. Overview of Events

3.1.1. Event of 9 May 1997

[11] On 9 May 1997, a pseudo-breakup occurred between 0519 UT and 0610 UT which was observed in both auroral activity and ground magnetometer data. During the pseudo-breakup, Polar was on an inbound orbit moving from the tail lobe into the plasma sheet. Figures 1a and 1b show ion and electron energy-time spectrograms from Polar. Both regions are easily identifiable and are labeled on the top of the first panel. Figure 1c shows electric field data. The weak electric field fluctuation starting at 0519 UT in the tail lobe which coincided with the onset (c.f. section 3.3), and the strong fluctuations encountered on entering the PSBL are the main topic of this paper.

[12] Figures 1d–1o show 12 UV images of auroral emission covering a time period of about 35 min. This sequence shows the spatiotemporal evolution of the aurora. Each image is a view of the Northern Hemisphere divided in MLT and ILAT. Polar's footprint is marked by a plus sign in each image. An auroral arc is first visible in Figure 1e. This time coincides with the onset time of a negative X bay at Gillam and Rabbit Lake ground stations (Figure 2). Polar's footprint traversed the most northern stations of the CANOPUS magnetometer network during this time period. In the following UV images (Figures 1g–1l), a typical auroral bulge can be seen to form, after which the aurora fades (Figures 1m–1o). The fading aurora coincides with the increasing X component in the ground magnetometer data (Figure 2), which indicates that the pseudo-breakup is in its recovery phase beginning at about 0542 UT. The X component of Gillam also shows strong oscillations in the Pi2 frequency range. These oscillations start at onset and last until the end of the expansion phase. During the recovery phase no similar oscillations were present.

3.1.2. Event of 23 May 1996

[13] The second event discussed in this paper occurred on 23 May 1996. The crossing of the tail lobe and the PSBL produced particle and field signatures (Figure 3) similar to those on 9 May 1997. Starting at about 0016 UT while in the tail lobe (see arrow), Polar recorded weak electric and magnetic field fluctuations (c.f. section 3.3), followed by large-amplitude fluctuations in the PSBL. The time of the first observed lobe fluctuations coincided with a ground

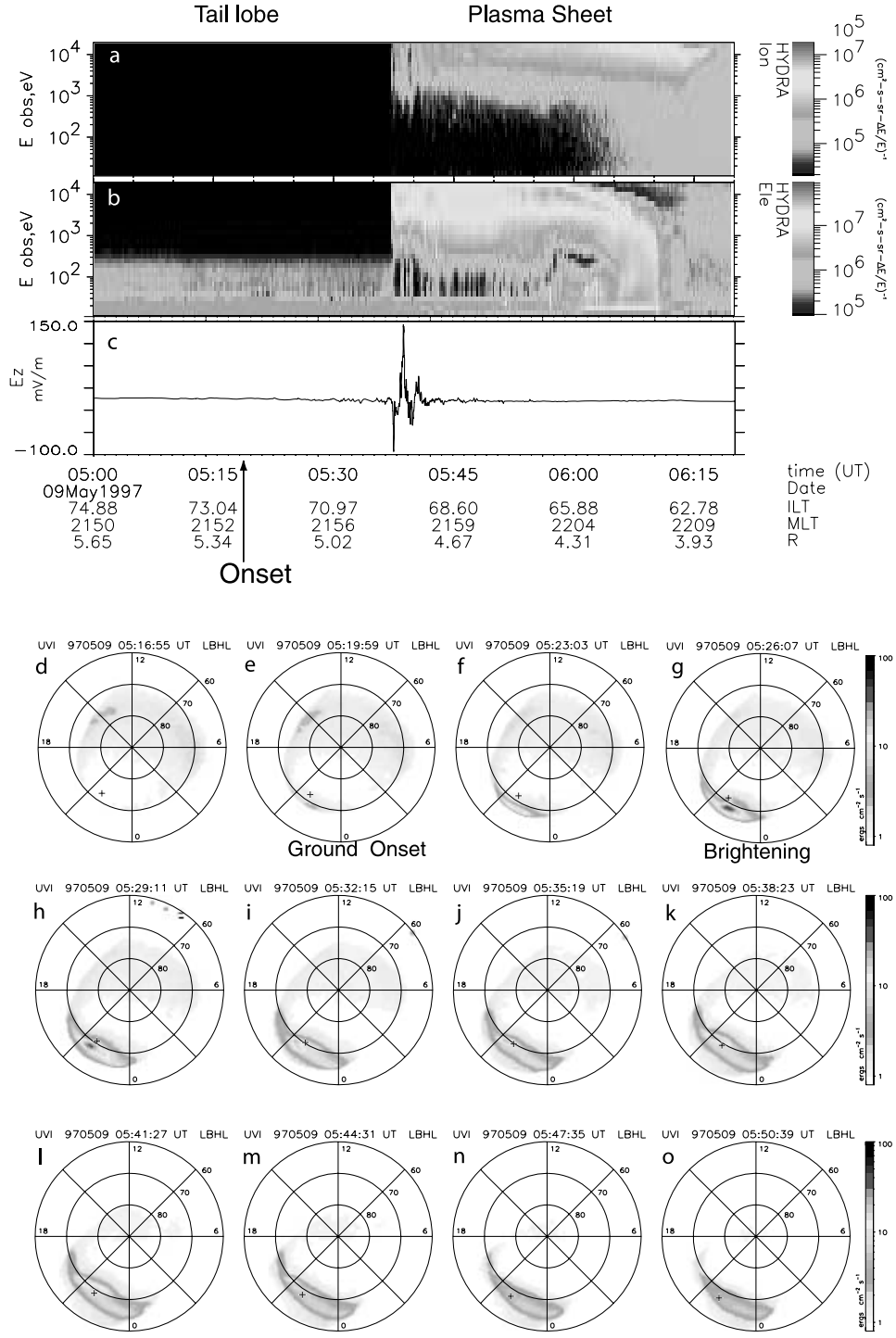

Figure 1. (a) Ion and (b) electron energy-time spectrograms and (c) electric field data on 9 May 1997 while Polar crossed the tail lobe and the plasma sheet. The time of substorm onset is indicated by an arrow. (d–o) Sequence of UV images taken on the same day. The development of an auroral bulge can be seen. In the second image an auroral arc forms (close to the plus sign), and the fourth image shows the onset of brightening.

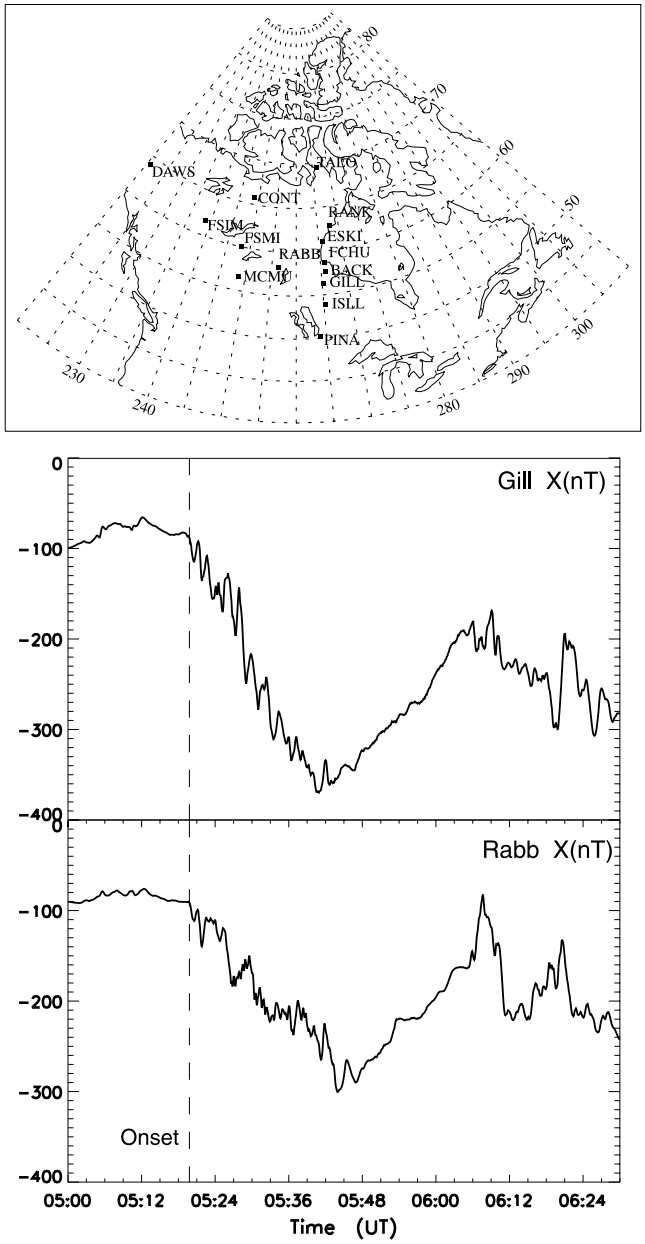

Figure 2. Map showing the geographic locations of the CANOPUS magnetometer stations. Beneath are magnetograms from Gillam and Rabbit Lake showing negative magnetic bays.

intensification of the X component as will be shown later. No UVI images were available to confirm the presence of auroral displays.

3.2. FACs

3.2.1. Event of 9 May 1997

[14] While in the tail lobe and the plasma sheet, Polar recorded the signatures of various FACs (labeled in Figure 4b) in the model-subtracted azimuthal magnetic field component, B_y. Also visible are large-amplitude perturbations in both magnetic and electric field (Figure 4a and 4b) which have been shown to be Alfvén waves [*Wygant et al.*, 2000]. The component, E_z, points northward (i.e., approximately along GSE z).

[15] The first FAC signature was recorded while Polar was in the tail lobe. Its onset coincided with the onset of the negative X bay recorded by CANOPUS (first dashed line from left in Figure 4c). Since the X component is associated with the substorm current wedge, it is possible that Polar did not record a local current sheet but instead the remote magnetic effect of the substorm current wedge.

[16] The second FAC is a local, upward directed current sheet. This is the direction of the statistical Region 1 current at the local time of about 2200 MLT. This current maps into the poleward region of the aurora (Figure 1g and thereafter). Note that the large-amplitude Alfvén waves were superposed onto this current.

[17] The next current sheet is downward and has the polarity of the Region 2 current. This current was not superposed with large Alfvén waves. It also maps into the aurora but at lower latitude (c.f. UV images of Figure 1).

[18] At about 0600 UT, the current direction changed once again to an upward current. This current lasted until 0608 UT while Polar was still in the plasma sheet. Comparison with magnetometer data at Gillam (second dashed line in Figure 4c) shows that the substorm current wedge current also ended at about the same time. It is thus possible that this in situ signature is associated, either remotely or locally, with the substorm current wedge current.

[19] After 0608 UT a small downward current can be seen. This downward current ends at about 0617 UT, which coincides with Polar leaving the electron plasma sheet (Figure 1).

3.2.2. Event of 23 May 1996

[20] The second event shows essentially the same FAC system (Figure 4e) as the 9 May 1997 event, and an Alfvén wave was also superposed onto the upward current in the PSBL [*Keiling et al.*, 2000].

[21] The ground data from Iqaluit (Figure 4f) are more variable in this event, which appears as a series of individual smaller intensifications. However, from 0016 UT (vertical dashed line) to about 0054 UT, a trend of a large-scale negative drop in the X component and an upward recovery thereafter can be identified. The ground onset at 0016 UT coincides with both the first observed FAC signature and the smaller-amplitude oscillations recorded by Polar in the tail lobe. This is similar to the previous event.

[22] In contrast to the 9 May 1997 event, we cannot identify a simultaneous ending of the ground recovery and an FAC signature at Polar's location.

3.3. Alfvén Waves in the Tail Lobes

3.3.1. Event of 9 May 1997

[23] At onset of the negative X bay on 9 May 1997, Polar, while in the tail lobe, observed small perturbations in the electric and magnetic fields, which started simultaneously with oscillations in ground magnetometer data from various stations (Figure 5).

[24] Figure 6 shows expanded views of two time intervals from Figure 5. Each view shows bandpass-filtered electric and magnetic field data from Polar together with CANOPUS magnetometer data for comparison. To better compare the phase relationships between E_z and B_y, Figures 6c and 6h show B_y and the Hilbert-transformed E_z overlaid. The Hilbert

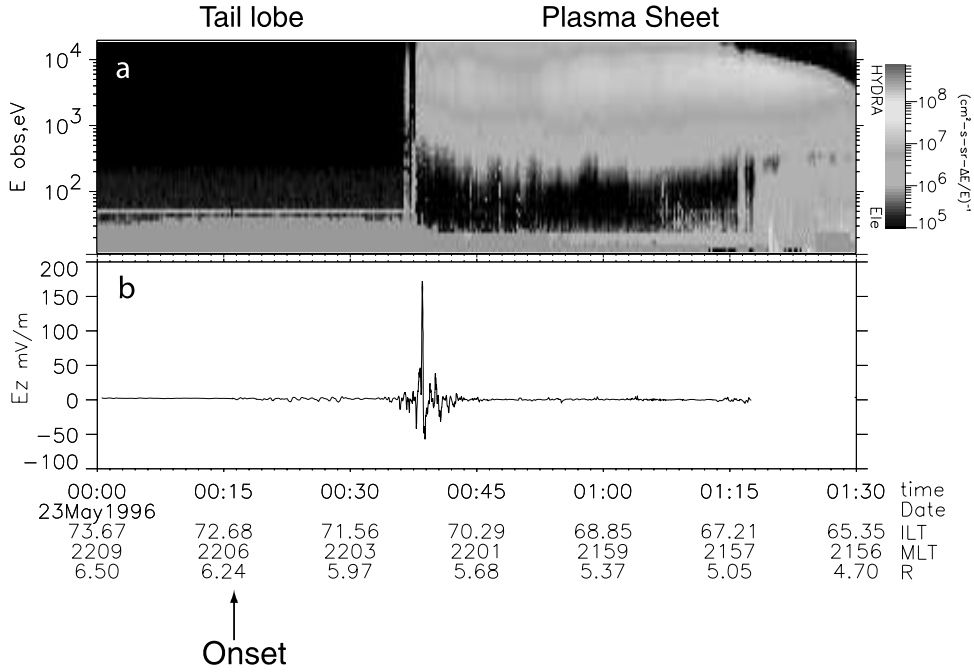

Figure 3. (a) Electron energy-time spectrograms and (b) electric field data on 23 May 1996 while Polar crossed the tail lobe and the plasma sheet. The time of substorm onset is indicated by an arrow.

transform shifts all frequency components by 90° without changing their amplitude [*Dubinin et al.*, 1990]. The fact that during some time intervals B_y and $H\{E_z\}$ are in phase means that these perturbations are standing Alfvén waves, most clearly seen in Figure 6h. This might come as a surprise since tail lobe field lines are open. However, once Alfvén waves begin to be reflected from the ionosphere, they will have the local structure of a standing Alfvén wave [*Wright et al.*, 1999]. The periods (frequencies) of the standing waves in Figures 6c and 6h are approximately 180 s (5.5 mHz) and 30 s (33 mHz), respectively.

[25] A comparison of ground data (Figure 6e and 6j) with B_y at Polar shows that similar oscillations were observed in space and on the ground, especially between 0521–0527 UT and 0531–0533 UT (see vertical dashed lines). Note that this implies that there is little or no Doppler shift in the Polar field measurements. Hence the tail lobe Alfvén waves had large perpendicular scale length. The observed in situ frequencies are therefore the real frequencies of the wave.

[26] In contrast to the standing waves, immediately poleward of the PSBL (0535–0536 UT), downward traveling Alfvén waves were recorded in the tail lobe (see dashed lines in Figures 6f and 6g). The Poynting flux calculations (Figures 6d and 6i) can also be used to identify standing and traveling characteristics. Furthermore, the Poynting flux values will later be compared with those of the PSBL Alfvén waves.

3.3.2. Event of 23 May 1996

[27] A comparison of tail lobe Alfvén waves and ground data for 23 May 1996 (Figure 7) yields similar results as for 9 May 1997. First, the tail lobe Alfvén waves show clear standing wave signatures at Polar's location, indicated by the 90° phase shift (Figure 7c; note that the Hilbert transform has shifted the signal by 90°), and, second, there is a very close match to the magnetic field oscillations recorded by the Iqaluit ground station (see vertical dashed lines in Figures 7b and 7e). The frequencies of both lobe waves and ground oscillations are the same. This again suggests large perpendicular scale length for the tail lobe Alfvén waves. Third, downward traveling lobe waves were also encountered immediately poleward of the PSBL. Fourth, the onset of the tail lobe Alfvén waves at Polar's location also coincided with the ground onset of both the oscillations and the negative drop of X (see Figures 4d–4f and Figure 7).

3.4. Alfvén Waves in the PSBL

3.4.1. Event of 9 May 1997

[28] Polar recorded large-amplitude Alfvén waves on entering the PSBL (Figures 1 and 4) which carried large amounts of Poynting flux and were conjugate to enhanced auroral luminosity. The Alfvén wave occurred during the expansion phase, i.e., the downward leg of the *X* bay (Figure 4c). In Figures 8a and 8b, an expanded view of these large-amplitude fields (filter range: 6s, 180 s) is shown. When overlaying E_z and B_y (Figure 8c), a phase shift is noticeable; in particular, the largest peaks in E_z and B_y (at ~0539 UT) do not coincide. This implies the interference of incident and reflected waves. We next investigate the frequency content and polarization of the large-amplitude Alfvén wave.

[29] A Fourier component analysis shows that two types of Alfvén waves are present: standing and traveling. The signals were bandpass filtered for different period ranges. For each period range we show E_z, B_y, E_z, and B_y (or $H\{B_y\}$) overlaid and the Poynting flux calculated from E_z and B_y (Figure 9). Depending on whether the component is a traveling or standing wave, the Hilbert transform was applied to B_y to facilitate comparison with E_z. The Alfvén

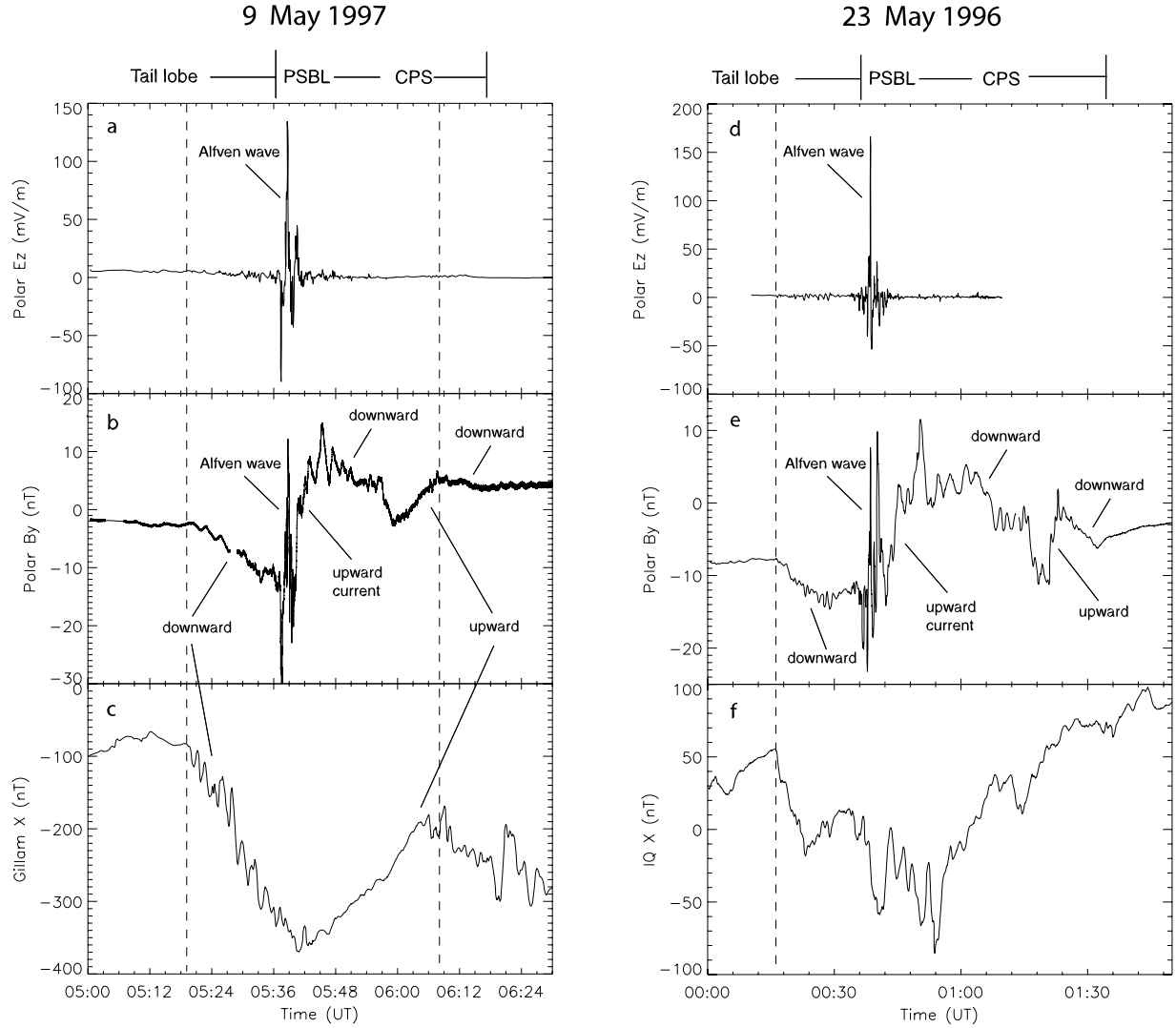

Figure 4. (a) Electric and (b) magnetic field data from Polar on 9 May 1997. Alfvén waves and field-aligned current (FAC) signatures are labeled. Above the first panel, the different plasma regions crossed by Polar are indicated. (c) The X component magnetic field data as recorded at Gillam is shown. The two vertical, solid lines are visual aides to emphasize the simultaneous beginning and ending of the in situ FAC and the magnetic bay at Gillam. (d–f) Similar to the previous three panels but for the 23 May 1996 event.

wave with the slowest variations (70–300 s) was a traveling wave since E_z and B_y are in phase. The E-to-B ratio of the main peaks is about 8000 km/s and is consistent with the Alfvén wave interpretation, and the Poynting flux is mostly downward. The next period range (40–67 s) shows standing Alfvén waves. E_z and $H\{B_y\}$ are in phase (or equivalently, E_z and B_y are in phase quadrature). The standing wave signature is also manifest in the alternating Poynting flux. The E-to-B ratio of the main peaks is about 6000 km/s. Note that this frequency range overlaps the Pi2 range. For a standing wave the E-to-B ratio is also largely dependent on how close the observation was made to the node or antinode of the electric and magnetic field, which could account for its smaller value.

[30] The next two period ranges (14–24 s and 9.5–12 s) show both earthward and tailward traveling Alfvén waves. Several peaks are present, resulting in a range of E-to-B ratios between 10,000 and 15,000 km/s. This range is possibly due to the fact that both earthward and tailward traveling waves are observed, which can change the E-to-B ratios.

[31] There is a possible trend that the peak E-to-B ratios of the different spectral components increased with smaller periods with the exception of the 40–67 s range (see above for an explanation). If we equate the smaller periods with smaller perpendicular size of the Alfvén waves, then this trend is consistent with the transition toward kinetic Alfvén waves [*Lysak and Lotko*, 1996].

[32] The spectral analysis also shows that most Poynting flux (larger by two orders of magnitude) was carried by the long-period traveling wave (70–300 s).

[33] Figure 10a shows power spectra of the electric and magnetic fields of the 9 May 1997 event in the frequency range from 4 mHz to 1 Hz. The electric and magnetic field follow power laws with slopes of −1.2 and −2.1, respectively.

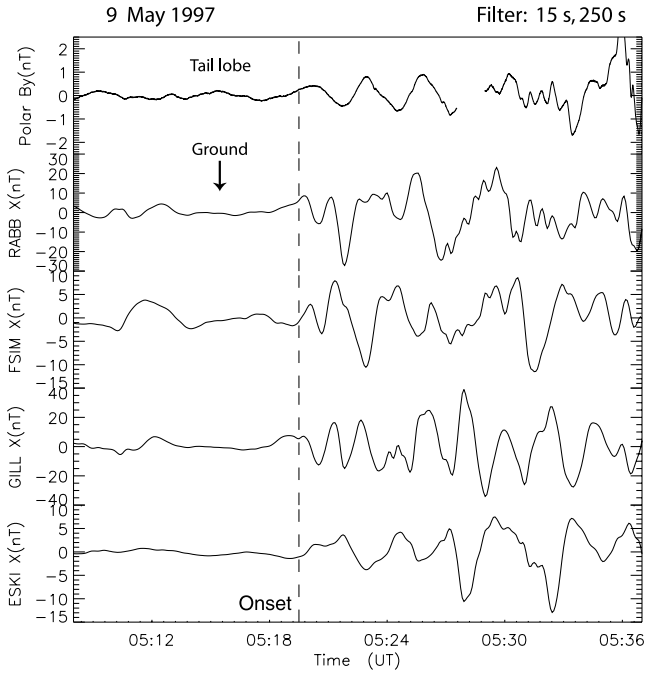

Figure 5. Comparison of the perturbation magnetic fields as measured by Polar and by four CANOPUS ground stations. Data were averaged (15 s) and detrended (250 s). At onset, as defined by the onset of the magnetic bay shown in Figure 2, Polar and ground stations simultaneously recorded the onset of oscillations. Polar was in the tail lobe at onset time.

[34] For selected time intervals, marked A, B, C, and D in Figure 9, hodograms of the magnetic field are shown in Figure 11 to investigate the polarization of the wave vector. The three-dimensional vector of B was transformed into a boundary-normal coordinate system [*Sonnerup and Cahill*, 1968]: BM and BL lie in the plane perpendicular to the wave normal. The direction of BL is approximately azimuthal and lies in the nominal plane of the plasma sheet boundary. The eigenvalues of the magnetic field variance matrix are well-separated so that the eigenvectors are not degenerate and the wave normal which is associated with the eigenvector of the smallest eigenvalue is well-determined. All waves show left-handed elliptical polarizations, such that the largest magnetic field perturbations lie in the plane of the plasma sheet boundary. For "D" there is also enhanced perturbation in the north-south direction, making this wave slightly less eliptically (more circularly) polarized. Assuming that the direction of the wave normal is identical with the direction of the wave vector, k, the angle between k and the 3-min average background magnetic field was less than 35°.

[35] In section 3.3 we showed that standing Alfvén waves in the tail lobe recorded by Polar were simultaneously detected on the ground. Similarly, we investigated whether the Alfvén waves recorded in the PSBL were also recorded on the ground. Using both power spectra and wave form comparisons (not shown), the data were not conclusive. Although wave power was present in both ground and space signals in the same frequency range, there were no matching peaks at one frequency. Furthermore, there was no direct correspondence in the ground and space signal waveforms as was clearly the case for the tail lobe waves. There might be a number of reasons for this: (1) The Polar spacecraft was not exactly conjugate to the ground stations, (2) the spacecraft data were Doppler-shifted, or (3) the traveling wave energy was dissipated before it reached the ionosphere (see also section 4.1).

3.4.2. Event of 23 May 1996

[36] Similar to the other event, the 23 May 1996 event shows large-amplitude Alfvén waves on entering the PSBL (Figures 3 and 4), carrying large Poynting flux in the direction of the ionosphere. The most important difference to the previous event is that no phase shift between the largest electric and magnetic field pulses is present (Figures 8d–8f). As a consequence, we find less reflected wave power in the various spectral components (Figure 12) compared to 9 May 1997. The three period ranges covering the range from 14 to 200 s show dominantly downward Poynting flux of comparable magnitude, although the Poynting flux of the slowest component (40–200s) dominates. The E-to-B ratios for the first three period ranges are about 9000, 18,000, and 18,000 km/s. The period range from 6 to 9 s shows both downward and upward directed Poynting flux of comparable magnitude with slight dominance in downward direction. Since several peaks are present, a range of E-to-B ratios is found: 10,000–20,000 km/s. As for the other event, we find that the peak E-to-B ratios of the lowest-frequency waves were smaller than those of the highest-frequency waves.

[37] Figure 10b shows power spectra of the electric and magnetic fields in the frequency range from 4 mHz to 1 Hz. These spectra follow power laws with slopes of −1.7 and −2.1, respectively. Whereas the exponent of the magnetic field is the same compared to the other event, the electric field exponent deviates. Nevertheless, these exponents (including those for the 9 May 1997 event) cover a range which is typical for low-frequency waves in the plasma sheet [*Maynard et al.*, 1982; *Bauer et al.*, 1995].

4. Summary and Discussion

[38] Here we reported the following properties of Alfvén waves (period range: 6–300 s in the spacecraft frame), which were observed in the tail lobe and the PSBL at geocentric distances of 5 to 6 R_E, and some associated phenomena:

[39] 1. Alfvén waves were excited in the tail lobes at substorm onset. Thus these ULF waves can be used as substorm indicator in the tail lobes.

[40] 2. The lobe waves showed both standing and traveling signatures: farther away from the PSBL, they were often standing; whereas immediately poleward of the PSBL, they were traveling downward.

[41] 3. The standing Alfvén waves in the tail lobe had large perpendicular scale sizes and were simultaneously recorded on the ground with almost identical waveforms.

[42] 4. Large-amplitude Alfvén waves in the PSBL occurred during the substorm expansion phase [*Keiling et al.*, 2000]. The waves showed standing and traveling signatures (both downward and upward).

[43] 5. The Poynting flux associated with the substorm-related Alfvén waves was two to three orders of magnitude larger in the PSBL than in the tail lobes.

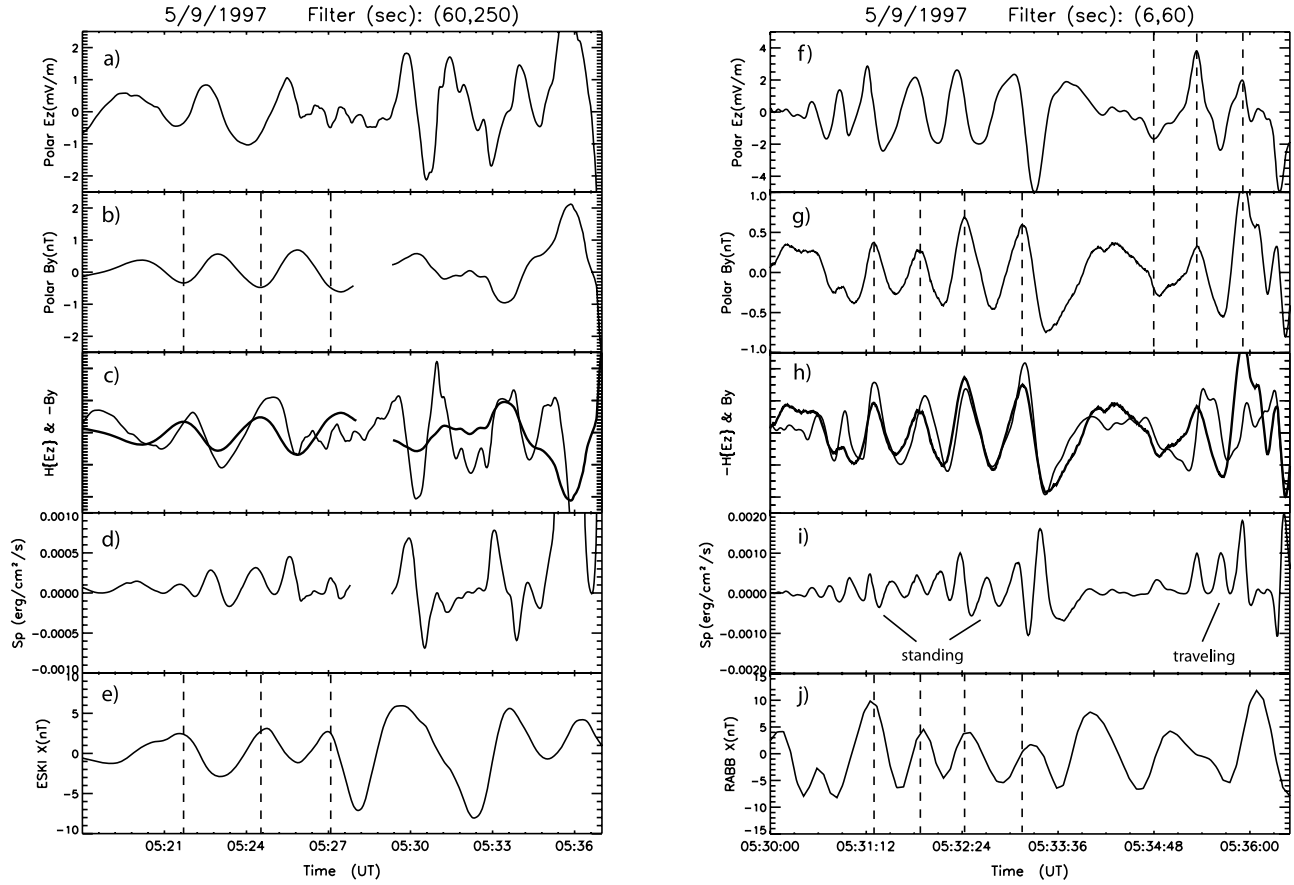

Figure 6. Comparison of Polar and ground data for two time intervals on 9 May 1997 while Polar was in the tail lobe. (a, b) Waveforms of the electric and magnetic components that are associated with shear Alfvén waves. (c) The magnetic field plotted together with the Hilbert-transformed electric field to emphasize standing wave signatures. (d) Poynting flux calculated from the fields shown in Figures 6a and 6b. (e) The *X* component of ESKI resembles the in situ magnetic field component, especially between 0521 and 0527 UT, suggesting that the in situ and the ground oscillations are caused by the same wave. (f–j) The same format as Figures 6a–6e. The standing Alfvén wave structure at Polar is very clear, and so is the similarity of in-situ magnetic field data and ground data at Rabbit Lake. At the end of the time interval while Polar was still in the lobe, an earthward traveling wave was recorded.

[44] 6. Most Poynting flux (>0.1 erg/cm^2/s in situ) was carried in downward traveling waves in the PSBL; one event (not shown) showed large Poynting flux in the standing wave components. However, waves which contain a large tailward Poynting flux component are rare compared to the earthward traveling waves. Furthermore, because of the standing wave nature of these waves, the net Poynting flux is near zero. For the events presented here the reflected Poynting flux was less by two orders of magnitude than the largest earthward directed Poynting flux. Reflected Poynting flux was observed in the period range 6–67 s with magnitudes <0.05 erg/cm^2/s.

[45] 7. A trend existed that for the highest-frequency waves the peak *E*-to-*B* ratio (i.e., Alfvén speed) was larger than for the lowest-frequency waves, which is consistent with a transition toward kinetic Alfvén waves, assuming higher frequency corresponds to smaller perpendicular sizes.

[46] 8. For the 9 May 1997, the PSBL Alfvén waves were left-hand elliptically polarized. The wave vector was within 35° of the background magnetic field, suggesting that the waves were phase mixed.

[47] 9. The large-amplitude, substorm-related PSBL Alfvén waves occurred in upward current regions.

[48] 10. The remote magnetic effect of the substorm current wedge current possibly accounted for the FAC signature in the tail lobe at Polar's location.

[49] These observations confirm and emphasize the role which Alfvén waves play in the substorm process. Furthermore, the properties of Alfvén waves identified here are important for the modeling of Alfvén waves in the magnetosphere to investigate generation mechanisms and wave-particle interactions on auroral field lines. In the following subsections, we discuss in more detail several aspects of our results.

4.1. Traveling and Standing Alfvén Waves

[50] Standing shear Alfvén waves on closed magnetic field lines are well-known phenomena. They are commonly referred to as FLR and ample observations of FLR exist in

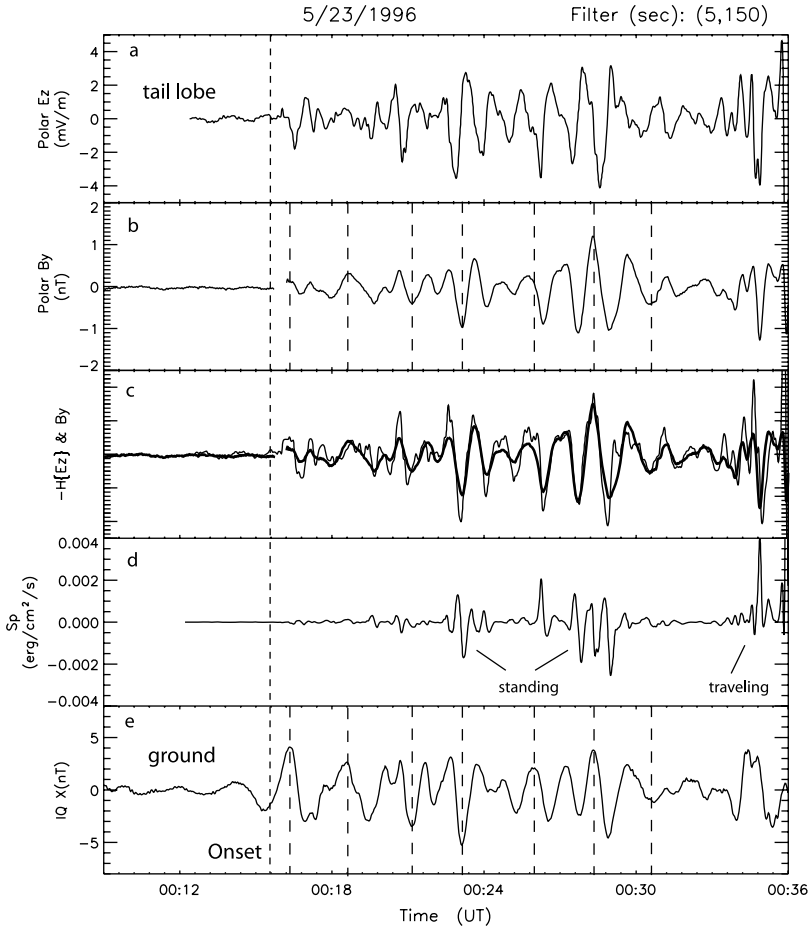

Figure 7. Comparison of Polar and ground data for a time interval on 23 May 1996 while Polar was in the tail lobe, using the same format as in Figure 6. The onset of the tail lobe Alfvén waves at Polar's location coincided with the onset of the ground oscillations (long dashed line). The tail lobe Alfvén waves show clear standing wave signatures at Polar's location, indicated by the 90° phase shift between E_z and B_y (c). The waveforms of the magnetic field oscillations recorded by (b) Polar and the (e) Iqaluit ground station are very similar (see vertical dashed lines). (d) In addition, earthward traveling lobe waves were encountered immediately poleward of the PSBL.

the magnetosphere [e.g., *Cahill et al.*, 1986; *Takahashi et al.*, 1988; *Anderson et al.*, 1990; *Lotko and Streltsov*, 1997]. We reported here standing Alfvén waves in the tail lobe which were associated with substorm onset. Since lobe field lines are open, the observed standing Alfvén waves in the lobe do not form FLR. The electric and magnetic field signatures of the lobe waves are the same as those of FLR but they do not represent an eigenmode of the field line. Instead, it is possible that lobe Alfvén waves reflected off the ionosphere superpose the incident waves at the satellite location to create the local standing wave signature [*Wright et al.*, 1999]. Standing Alfvén waves were recently reported in the tail lobes by *Ober et al.* [2001] and *Keiling et al.* [2001] without further characterization.

[51] However, we also reported earthward traveling Alfvén waves in the tail lobe which occurred preferentially adjacent to the PSBL. These waves are consequently absorbed below the satellite. Whereas Alfvén waves traveling on PSBL field lines have several locations to be reflected and absorbed (see below), lobe Alfvén waves interact with the ionosphere. It is uncertain at this point why these near-PSBL lobe waves are different from the standing lobe waves farther away from the outer edge of the PSBL. It appears that there is a transition layer between the dissipative PSBL and the nondissipative lobes, which acts dissipatively on these waves.

[52] We also showed standing wave signatures in the period range between 40 and 67 s associated with large-amplitude Alfvén waves in the PSBL. Although PSBL field lines are closed, we have not confirmed whether the standing waves are FLR. Because the PSBL is a very dynamic region with field lines threading the high-β magnetotail, it is more likely that the standing waves were not FLR but were the result of the superposition of incident and reflected waves (similar to the lobe waves). In the range 6–24 s, incident and reflected waves were often spatially separated so as to not interfere at Polar's location.

[53] Our results can be compared to the study of *Nagatsuma et al.* [1996], who investigated properties of low-altitude Alfvén waves (3000 to 10,000 km using Akebono) at the poleward border of the auroral zone in

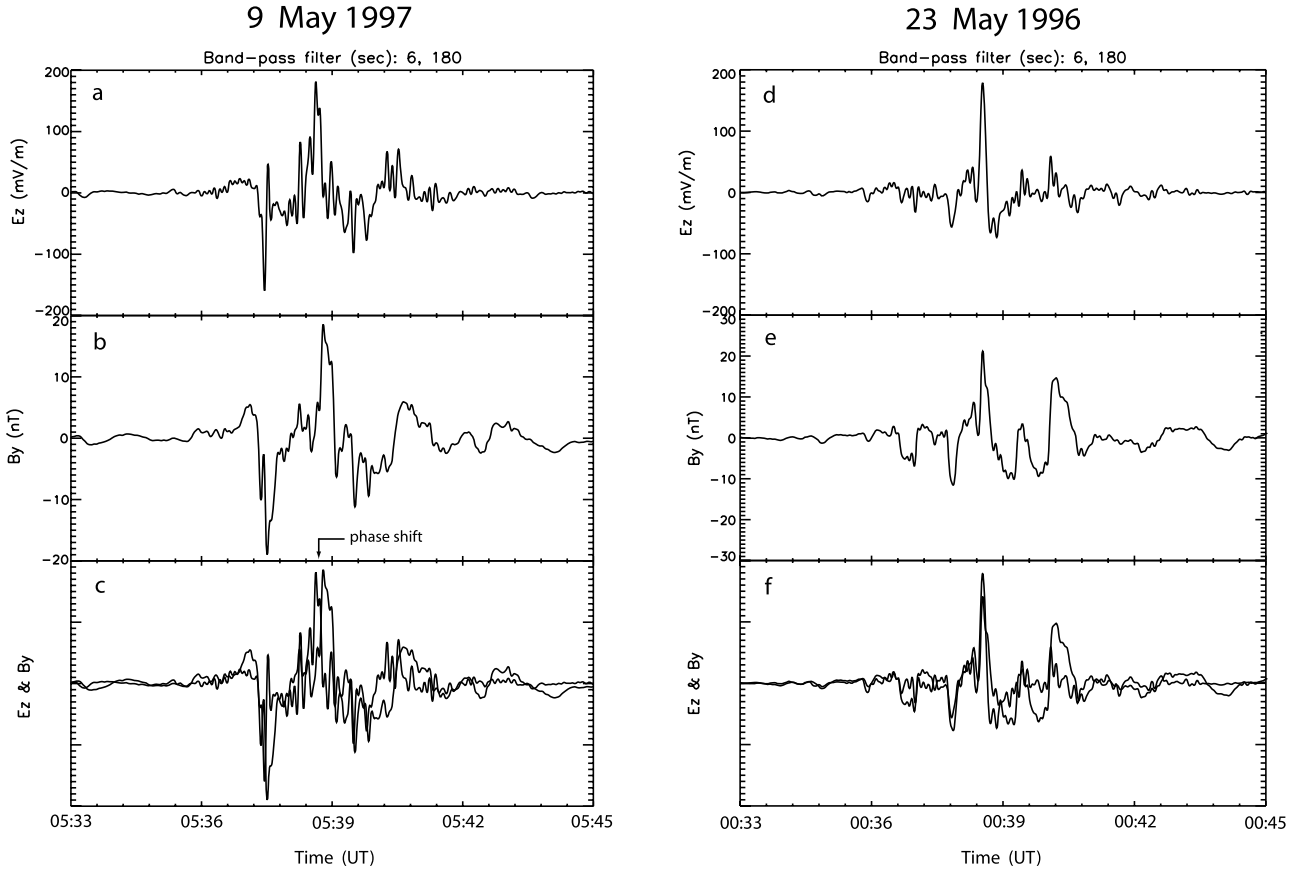

Figure 8. Phase-shift comparison of the (a) electric and (b) magnetic field components (perpendicular to each other) of the large-amplitude Alfvén waves observed on 9 May 1997 in the PSBL (previously reported by *Wygant et al.* [2000]). (c) E_z and B_y overlaid. The phase shift indicates that a mixture of traveling and standing waves are present. (d–f) Same as the previous three panels for the 23 May 1996 event (previously reported by *Keiling et al.* [2000]). The main difference is that no phase shift between the largest E_z and B_y peaks exists.

a similar frequency band as used in our study. It was shown that for the period range (12–384 s) most of the downward traveling Alfvén wave energy is reflected, presumably off the ionosphere, causing incident and reflected waves to interfere. Both reflected and incident Poynting fluxes were of nearly equal amplitude (slight dominance by the downward Poynting flux). Thus the large, and mostly earthward directed, Poynting flux as recorded by Polar at 5 to 6 R_E is not observed at Akebono's altitude suggesting its dissipation at altitudes between Polar and Akebono. This dissipation of electromagnetic energy can potentially result in the acceleration of electrons, which in turn cause auroral displays [*Wygant et al.*, 2000]. This scenario is supported by a statistical study that shows that the net Poynting flux (including all frequency components) at 4 to 7 R_E traveling toward the Earth is correlated to conjugate energy flux of ionospheric electron precipitation causing auroral luminosity [*Keiling et al.*, 2002].

[54] The difference in Poynting flux at Akebono's and Polar's altitudes are also consistent with the simulation results by *Streltsov and Lotko* [2003], where it was shown that substantial wave Poynting flux is dissipated in the anomalous resistive layer [*Lysak and Dum*, 1983]. Using numerical simulations, the dependence of Alfvén wave reflection and absorption in the low-altitude magnetosphere on several parameters (amplitude, frequency, and perpendicular scale size) were investigated. ULF waves with frequencies between 0 and 0.1 Hz (which is similar to our study), and perpendicular scales of 4–40 km mapped to the ionosphere were investigated. It was found that both larger-amplitude and lower-frequency waves are preferably absorbed in the anomalous resistive layer. Hence it is possible that the Akebono satellite was below this layer and therefore did not record large-amplitude, low-frequency Alfvén waves as recorded by Polar. We point out that another region of reflection of earthward traveling PSBL Alfvén waves above Akebono's altitudes are parallel electric fields in the auroral zone [*Vogt and Haerendel*, 1998].

[55] One uncertainty in the comparison of our study with *Nagatsuma et al.*'s [1996] study is that these authors did not comment on the geomagnetic activity level prevailing during their events. Since it was shown in a Polar study that during quiet times Alfvén waves are also present in the PSBL at 4–7 R_E but with much smaller amplitudes [*Keiling et al.*, 2002], it is not known whether large-amplitude

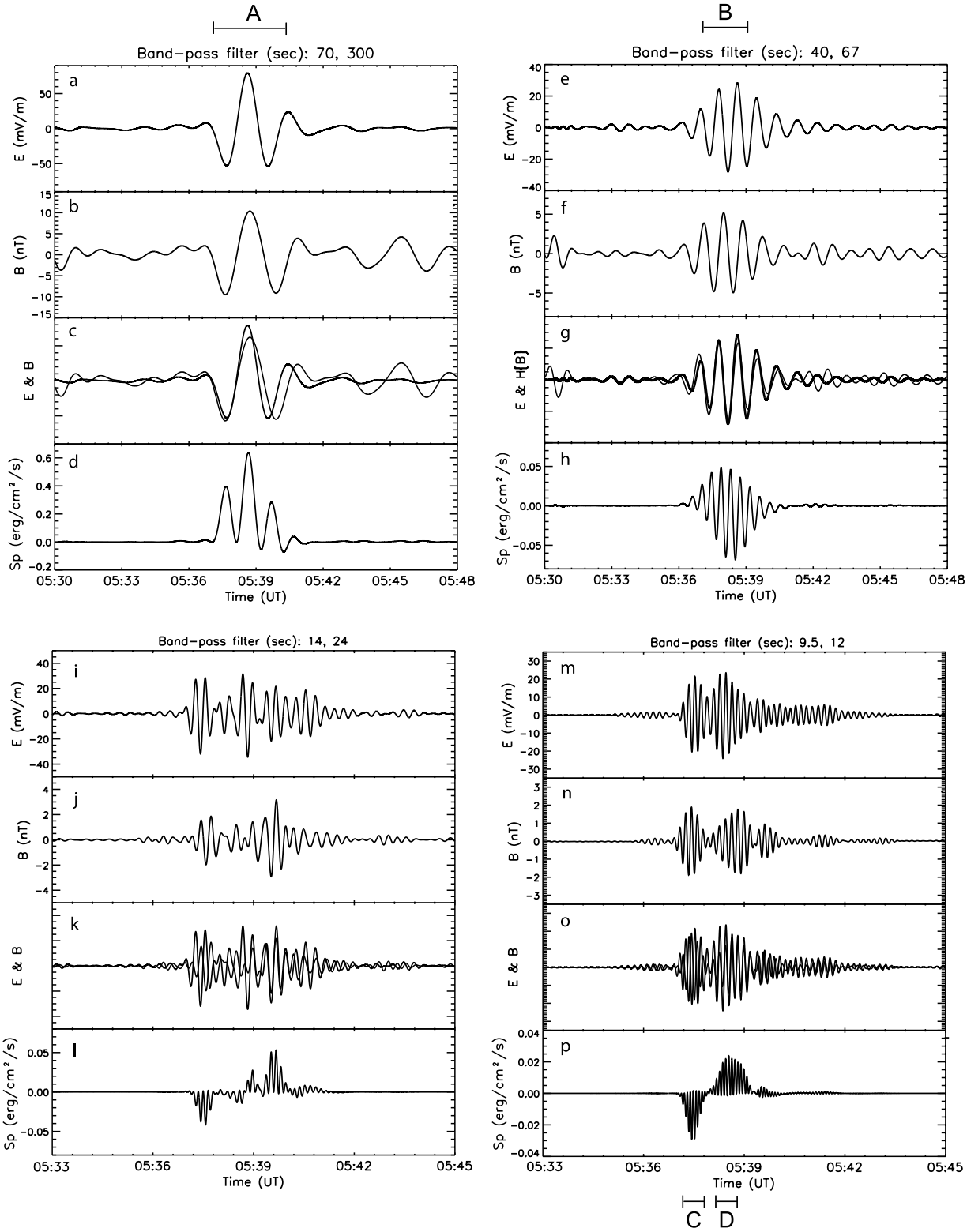

Figure 9. Four spectral components of the signal shown in Figures 8a and 8b (9 May 1997). For each component, (a) the electric field, E_z, (b) the magnetic field, B_y, (c) the electric and magnetic field (or Hilbert-transformed magnetic field) overlaid, and (d) the Poynting flux calculated from the two field components (Figures 9a and 9b) are shown. The first (Figures 9a–9d), third (Figures 9i–9l) and fourth (Figures 9m–9p) spectral components show traveling waves, whereas the second (Figures 9e–9h). spectral component shows a standing wave signature since E_z and $H(B_y)$ are in phase (or, equivalently, E_z and B_y are in phase quadrature).

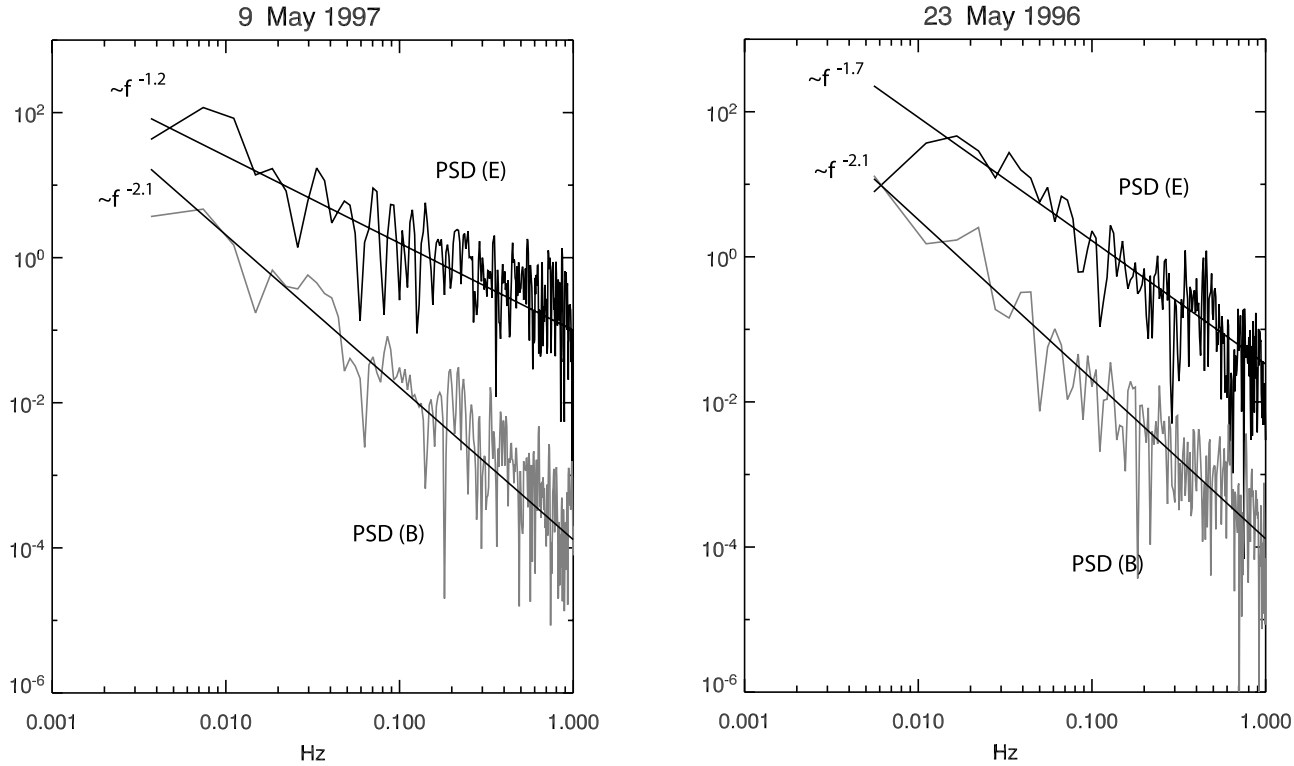

Figure 10. (a) Power spectra of the electric and magnetic fields (shown in Figures 8a and 8b). (b) Power spectra of the electric and magnetic fields (shown in Figures 8d and 8e).

Alfvén waves were present at higher altitude (4–7 R_E) during the events studied by *Nagatsuma et al.* [1996].

[56] Finally, we caution the reader to interpret the quoted frequencies (periods) of the observed PSBL Alfvén waves as the true values in the Earth frame. Because of steep density gradients at the outer edge of the PSBL (which is the region where the Alfvén waves were observed), Alfvén waves phase mix and obtain a smaller perpendicular size than the lobe Alfvén waves [*Allan and Wright*, 2000]. This smaller perpendicular size and the relative motion of Polar and the PSBL make the determination of the Alfvén wave frequency in the Earth frame uncertain. It is, on the other hand, notable that *Nagatsuma et al.* [1996] came to the conclusion that electric and magnetic field fluctuations in the period range below 384 s are Alfvén waves, whereas above they are static FACs. This agrees with our results as far as the Alfvén wave interpretation is concerned. Because Akebono and Polar traversed the auroral field lines at very different altitudes with different speeds, this could mean that the waves at Polar's and Akebono's altitudes might only be Doppler-shifted by small amounts so as to not significantly change the measured frequency from the Earth-frame frequency. For the lobe Alfvén waves, in fact, we could show that the measured frequency was close to the true frequency (i.e., little or no Doppler shift), which was based on comparisons to ground oscillations.

4.2. FACs and Alfvén Waves

[57] An important correlation reported here is the simultaneous presence of both FAC and Alfvén waves. It is possible that the current signature, which started simultaneously with the lobe Alfvén waves, was the remote effect of the substorm current wedge and not a local current. The local plasma in the tail lobe is generally too tenuous and cold to support such a current. (If there was a current-carrying particle population in the lobe, then its energy was below the threshold of the particle instrument (12 eV) used in this study.) The magnetic field due to this remote source would thus be curl-free. The main reason for this interpretation is the fact that both the ground onset of the negative leg of the magnetic substorm bay and the in situ FAC signature occurred simultaneously. Such a tail lobe signature of the substorm current wedge has been reported before by *Jacquey et al.* [1991] in association with a tailward propagating current disruption. Interestingly, the recovery of the ground magnetic bay was possibly also observed by Polar while in the CPS.

[58] Recently, *Ober et al.* [2001] reported electric and magnetic field oscillations in the tail lobe which had a similar frequency compared to simultaneous ground oscillations. The lobe oscillations also started together with a current signature (slope of B_y). These observations are similar to ours. However, the authors gave a different interpretation for the oscillations and the current signature. Their interpretation was that the spacecraft entered a spatial boundary with fringing electric fields causing the oscillations.

[59] The current signature in the PSBL, on the other hand, is clearly due to a local FAC, i.e., the current was carried by particles. This FAC was followed by an FAC in the opposite direction. This current pattern has been reported at low altitude and high altitude [e.g., *Carlson et al.*, 1998; *Schriver et al.*, 2003]. For three other large-amplitude

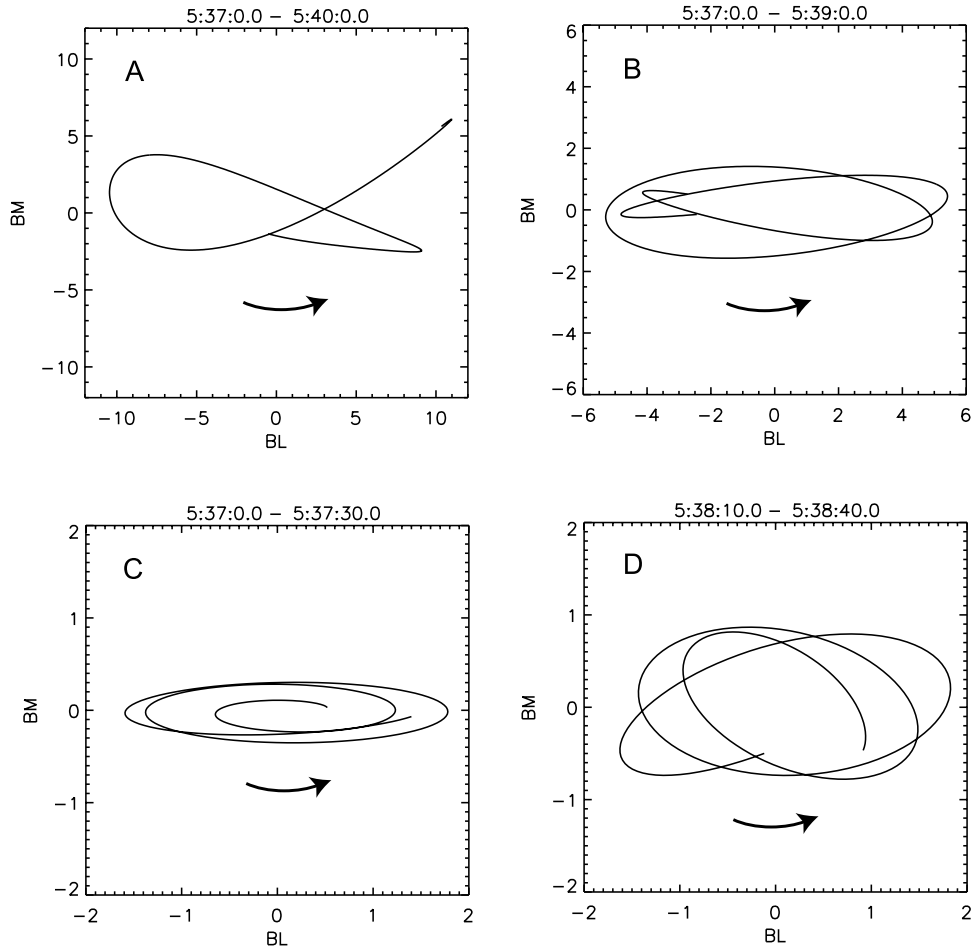

Figure 11. Hodogram representation of the magnetic field for time intervals marked by A, B, C, and D in Figure 9 for the 9 May 1997 event. BM and BL lie in the plane perpendicular to the wave normal.

Alfvén wave events (not shown here), we found that the Alfvén waves occurred in the upward current region (primary current). Other studies have shown large electric field structures in the return current region (downward current), which were shown to be static structures [*Marklund et al.*, 2001; *Johansson et al.*, 2004]. It is thus possible that there exists a causal connection between Alfvén waves and the primary current region and between quasi-static structures and the return current region. However, our event database is too small to draw definite conclusions.

[60] *Nagatsuma et al.* [1996] reported the superposition of Alfvén waves and FAC for 31 events at the polar edge of the auroral region at low altitude (<9000 km). Their observations were similar to ours. The authors also argued that a causal connection between Alfvén waves and these boundary currents exists (see also section 4.4).

4.3. Alfvén Waves at Substorm Onsets

[61] It has been shown previously that Alfvén waves occur at substorm onset in the plasma sheet and the plasmasphere [e.g., *Takahashi et al.*, 1988; *Osaki et al.*, 1998; *Toivanen et al.*, 2003]. Our observations here extend these findings by showing that Alfvén waves in the tail lobe can also occur simultaneously with substorm onset. It is thus suggested that these tail lobe waves can be used as a new additional indicator for substorm onset.

[62] We note that it has also been argued that some FLR Alfvén waves in the frequency range from 1 to 4 mHz can be the initiator of substorm onset which implies that they occur before substorm onset [*Samson et al.*, 1992].

4.4. Alfvén Wave Generation

[63] Mode coupling of fast mode and Alfvén waves has been shown to exist in the magnetosphere (dayside magnetosphere and the CPS), and many simulation studies have also shown its effectiveness [e.g., *Rankin et al.*, 1993, 1994; *Allan and Wright*, 1998, 2000; *Lee and Lysak*, 1999]. A first requirement for the mechanism is the existence of fast mode waves. It is generally agreed that the reconfiguration of the magnetotail during a substorm will generate compressional MHD waves and observational evidence exists as well [e.g., *Bauer et al.*, 1995; *Sigsbee et al.*, 2002]. These waves can then travel to different regions in the magnetotail. *Liu et al.* [1995] consider a scenario where compressional energy from substorm processes near the center of the magnetotail couples to shear Alfvén waves in the region of strong Alfvén velocity gradients in the PSBL. Similarly, *Samson et al.* [1991] show field line resonances near the inner

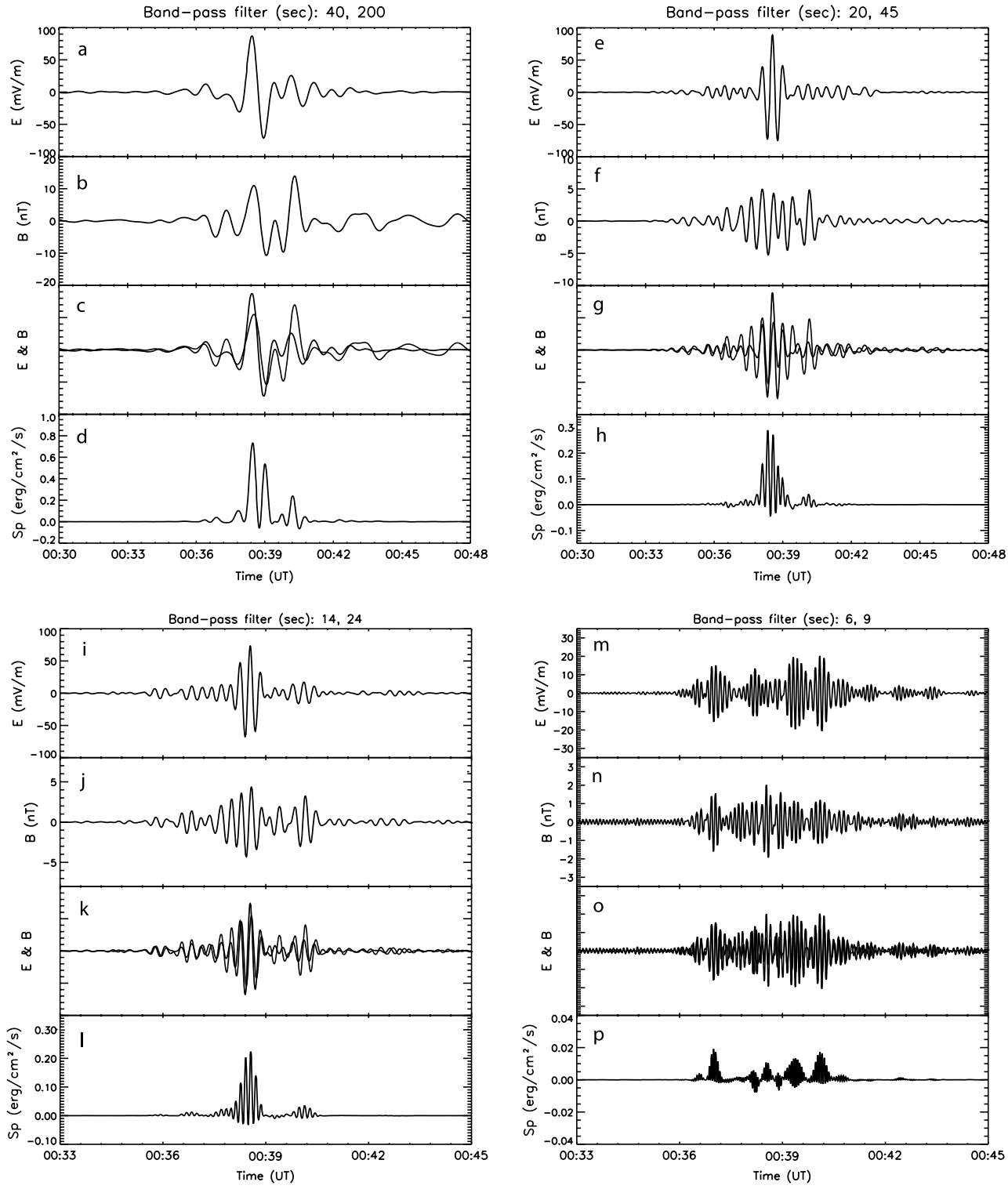

Figure 12. Four spectral components of the signal shown in Figures 8d and 8e (23 May 1996). Same format as in Figure 9. (a–l) The first three spectral components show dominantly downward traveling waves, whereas (m–p) the last spectral component shows both incident and reflected waves.

boundary of the plasma sheet and use the same argument. *Allan and Wright* [2000] simulated an MHD wave guide and showed that shear Alfvén waves are generated in the PSBL and the tail lobe.

[64] Here we reported Alfvén waves in the tail lobes and the PSBL, and thus it is suitable to compare our observations with the simulation results by *Allan and Wright* [2000]. First, Allen and Wright predicted that the lobe

waves would have large perpendicular scales. Our observations of lobe Alfvén waves were in good agreement with these simulation results. Second, Allen and Wright concluded that only a small fraction of the fast mode energy couples to both the lobe and the PSBL Alfvén waves. Here we demonstrated that tail lobe field lines indeed carried only small Poynting flux compared to the 2–3 orders of magnitude larger PSBL Alfvén waves. This large Poynting flux difference, however, raises the question of whether the waves in both regions are generated by the same mechanism. The largest Alfvén waves observed in the PSBL show electric field amplitudes >100 mV/m at about 5 R_E, whereas in the tail lobe they are of the order of a few mV/m. These smaller amplitudes can be coupled via fast mode waves as simulated and observed in the magnetosphere. The large-amplitude waves, on the other hand, are probably not coupled directly with fast mode waves. Instead, *Streltsov et al.* [2002] showed in a numerical study that these large-amplitude Alfvén waves can result from initially smaller Alfvén waves in the magnetotail and subsequent propagation along the magnetic field lines located on steep density gradients as found in the PSBL. A requirement for generating large amplitudes comparable to the Polar observations was the presence of an anomalous resistive layer in the simulation. We note, however, that their study did not simulate the coupling of fast mode waves and Alfvén waves, but instead smaller amplitude Alfvén waves were simply driven in the magnetotail.

[65] Alternatively, we noted that the largest Alfvén waves observed in the PSBL occurred in concert with FAC. *Nagatsuma et al.* [1996] also noted this fact at much lower altitude (<9000 km). These authors thus suggested that the Alfvén waves are indeed driven by the FAC. Other scenarios are also possible, such as reconnection [e.g., *Song and Lysak*, 1989, 2001], since the PSBL Alfvén wave travel on field lines closest to the open-closed field line boundary which presumably maps into the reconnection region. Whereas mode-coupling has been firmly established for the generation of some small-amplitude Alfvén waves, the generation mechanism of the largest of them is still speculative because too many excitation mechanisms are still possible. Nevertheless, we hope that some of the spectral properties of Alfvén waves presented here will help theoretical and numerical work in finding the generation mechanism (or possibly several) that operate in the PSBL.

[66] **Acknowledgments.** We thank Robert Lysak and Yan Song for useful discussions and Mark Engebretson for a critical reading of the manuscript. Analysis of electric field data was supported by NASA International Solar Terrestrial Program (NASA contract NAG 5-3182). Analysis of magnetometer data was supported by NASA grant NAG 5-7721. The work of Anatoly Streltsov was supported by NASA grant NNG04GE22G. We thank Craig Kletzing for providing the Hydra particle data. The CANOPUS project is supported by the Canadian Space Agency. We thank John Samson for the CANOPUS data. We also thank Larry Newitt for providing Iqaluit ground data from the Geological Survey of Canada.

[67] Shadia Rifai Habbal thanks Andrew N. Wright and Tsutomu Nagatsuma for their assistance in evaluating this paper.

References

Alfvén, H. (1942), Existence of electromagnetic-hydromagnetic waves, *Nature*, *150*, 405.

Allan, W., and A. N. Wright (1998), Hydromagnetic wave propagation and coupling in a magnetotail waveguide, *J. Geophys. Res.*, *103*, 2359.

Allan, W., and A. N. Wright (2000), Magnetotail waveguide: Fast and Alfvén waves in the plasma sheet boundary layer and lobe, *J. Geophys. Res.*, *105*, 317.

Anderson, B. J., et al. (1990), A statistical study of Pc 3–5 pulsations observed by the AMPTE/CCE magnetic fields experiment: 1. Occurrence distributions, *J. Geophys. Res.*, *95*, 10,495.

Bauer, T. M., et al. (1995), Low-frequency waves in the near-Earth plasma sheet, *J. Geophys. Res.*, *100*, 9605.

Cahill, L. J., et al. (1986), Electric and magnetic observations of the structure of standing waves in the magnetosphere, *J. Geophys. Res.*, *91*, 8895.

Carlson, C. W., et al. (1998), FAST observations in the downward current region: Energetic upgoing electron beams, parallel potential drops, and ion heating, *Geophys. Res. Lett.*, *25*, 2017.

Chaston, C. C., et al. (2000), Alfvén waves, density cavities and electron acceleration observed from the FAST spacecraft, *Phys. Scr. T*, *84*, 64.

Chaston, C. C., et al. (2003), Properties of small-scale Alfvén waves and accelerated electrons from FAST, *J. Geophys. Res.*, *108*(A4), 8003, doi:10.1029/2002JA009420.

Dubinin, E. M., P. L. Israelevich, and N. S. Nikolaeva (1990), Auroral electromagnetic disturbances at an altitude of 900 km: The relationship between the electric and magnetic field variations, *Planet. Space. Sci.*, *38*, 97.

Goertz, C. K. (1984), Kinetic Alfvén waves on auroral field lines, *Planet Space Sci.*, *32*, 1387.

Harvey, P., et al. (1995), The electric field instrument on the Polar satellite, *Space Sci. Rev.*, *71*, 583.

Jacquey, C., et al. (1991), Location and propagation of the magnetotail current disruption during substorm expansion: Analysis and simulation of an ISEE multi-onset event, *Geophys. Res. Lett.*, *18*, 389.

Johansson, T., et al. (2004), Intense high-altitude auroral electric fields – temporal and spatial characteristics, *Ann. Geophys.*, *22*, 2485.

Keiling, A., et al. (2000), Large Alfvén wave power in the plasma sheet boundary layer during the expansion phase of substorms, *Geophys. Res. Lett.*, *27*, 3169.

Keiling, A., et al. (2001), Properties of large electric fields in the plasma sheet at 4–7 RE measured with Polar, *J. Geophys. Res.*, *106*, 5779.

Keiling, A., et al. (2002), Correlation of Alfvén wave Poynting flux in the plasmas sheet at 4–7 R_E with ionospheric electron energy flux, *J. Geophys. Res.*, *107*(A7), 1132, doi:10.1029/2001JA900140.

Keiling, A., et al. (2003), Global morphology of wave Poynting flux: Powering the aurora, *Science*, *299*, 383.

Knudsen, D. J., et al. (1992), Alfvén waves in the auroral ionosphere: A numerical model compared with measurements, *J. Geophys. Res.*, *97*, 77.

Lee, D.-H., and R. Lysak (1999), MHD waves in a three-dimensional dipolar magnetic field: A search for Pi2 pulsations, *J. Geophys. Res.*, *104*, 28,691.

Liu, W. W., et al. (1995), Theory and observation of auroral substorms: A magnetohydrodynamic approach, *J. Geophys. Res.*, *100*, 79.

Lotko, W., and A. V. Streltsov (1997), Magnetospheric resonance, auroral structure and multipoint measurements, *Adv. Space Res.*, *20*(4/5), 1067.

Lysak, R. L. (1990), Electrodynamic coupling of the magnetosphere and ionosphere, *Space Sci. Rev.*, *52*, 33.

Lysak, R. L., and C. T. Dum (1983), Dynamics of magnetosphere-ionosphere coupling including turbulent transport, *J. Geophys. Res.*, *88*, 365.

Lysak, R. L., and W. Lotko (1996), On the dispersion relation for shear Alfvén waves, *J. Geophys. Res.*, *101*, 5085.

Mallinckrodt, A. J., and C. W. Carlson (1978), Relations between transverse electric fields and field-aligned currents, *J. Geophys. Res.*, *83*, 1426.

Marklund, G., et al. (2001), Temporal evolution of the electric field accelerating electrons away from the auroral ionosphere, *Nature*, *414*, 724.

Maynard, N. C., et al. (1982), Turbulent electric fields in the nightside magnetosphere, *J. Geophys. Res.*, *87*, 1445.

Morooka, M., et al. (2004), Cluster observations of ULF waves with pulsating electron beams above the high latitude dusk-side auroral region, *Geophys. Res. Lett.*, *31*, L05804, doi:10.1029/2003GL017714.

Nagatsuma, T., et al. (1996), Field-aligned currents associated with Alfvén waves in the poleward boundary region of the nightside auroral oval, *J. Geophys. Res.*, *101*, 21,715.

Ober, D. M., et al. (2001), Electrodynamics of the poleward auroral border observed by Polar during a substorm on April 22, 1998, *J. Geophys. Res.*, *106*, 5927.

Osaki, H., et al. (1998), Pi2 pulsations observed from the Akebono satellite in the plasmasphere, *J. Geophys. Res.*, *103*, 17,605.

Rankin, R., et al. (1993), Simulations of driven field line resonances in the Earth's magnetosphere, *J. Geophys. Res.*, *98*, 21,341.

Rankin, R., et al. (1994), Nonlinear standing shear Alfvén waves in the Earth's magnetosphere, *J. Geophys. Res.*, *99*, 21,291.

Rostoker, G., et al. (1995), Canopus—A ground-based instrument array for remote sensing the high latitude ionosphere during the ISTP/GGS program, *Space Sci. Rev.*, *71*, 743.

Russell, C. T., et al. (1995), The GGS/Polar Magnetic Fields Investigation, *Space Sci. Rev.*, *71*, 563.

Samson, J. C., et al. (1991), Observations of a detached, discrete arc in association with field line resonances, *J. Geophys. Res.*, *96*, 15,683.

Samson, J. C., et al. (1992), Substorm intensifications and field line resonances in the nightside magnetosphere, *J. Geophys. Res.*, *97*, 8495.

Schriver, D., et al. (2003), FAST/Polar conjunction study of field-aligned auroral acceleration and corresponding magnetotail drivers, *J. Geophys. Res.*, *108*(A9), 8020, doi:10.1029/2002JA009426.

Scudder, J., et al. (1995), HYDRA—A 3-dimensional electron and ion hot plasma instrument for the Polar spacecraft of the GGS mission, *Space Sci. Rev.*, *71*, 459.

Sigsbee, K., et al. (2002), Geotail observations of low-frequency waves and high-speed earthward flows during substorm onsets in the near magnetotail from 10 to 13 R_E, *J. Geophys. Res.*, *107*(A7), 1141, doi:10.1029/2001JA000166.

Song, Y., and R. Lysak (1989), Current dynamo effect of 3-D time-dependent reconnection in the dayside magnetopause, *Geophys. Res. Lett.*, *16*, 911.

Song, Y., and R. Lysak (2001), Towards a new paradigm: From a quasi-static description to a dynamical description of the magnetosphere, *Space Sci. Rev.*, *95*, 273.

Sonnerup, B. U. Ö., and L. J. Cahill (1968), Explorer 12 Observations of the magnetopause current layer, *J. Geophys. Res.*, *73*, 1757.

Streltsov, A. V., and W. Lotko (2003), Reflection and absorption of Alfvénic power in the low-altitude magnetosphere, *J. Geophys. Res.*, *108*(A8), 8016, doi:10.1029/2002JA009425.

Streltsov, A. V., W. Lotko, A. Keiling, and J. R. Wygant (2002), Numerical modeling of Alfvén Waves observed by the POLAR spacecraft in the nightside plasma sheet boundary layer, *J. Geophys. Res.*, *107*(A4), 1173, doi:10.1029/2001JA000233.

Takahashi, K., et al. (1988), AMPTE/CCE observations of substorm-associated standing Alfvén waves in the midnight sector, *Geophys. Res. Lett.*, *15*, 1287.

Toivanen, P. K., et al. (2003), Polar observations of transverse magnetic pulsations initiated at substorm onset in the high-latitude plasma sheet, *J. Geophys. Res.*, *108*(A7), 1267, doi:10.1029/2001JA009141.

Torr, M. R., et al. (1995), A far ultraviolet imager for the International Solar-Terrestrial Physics Mission, in *The Global Geospace Mission*, pp. 459–495, Springer, New York.

Vogt, J., and G. Haerendel (1998), Reflection and transmission of Alfvén waves at the auroral acceleration region, *Geophys. Res. Lett.*, *25*, 277.

Wright, A. N., et al. (1999), Phase mixing and phase motion of Alfvén waves on tail-like and dipole-like magnetic field lines, *J. Geophys. Res.*, *104*, 10,159.

Wygant, J. R., et al. (2000), Polar spacecraft based comparison of intense electric fields and Poynting flux near and within the plasma sheet-tail lobe boundary to UVI images: An energy source for the Aurora, *J. Geophys. Res.*, *105*, 18,675.

Wygant, J. R., et al. (2002), Evidence for kinetic Alfvén waves and parallel electron energization at 5–7 R_E altitudes in the plasma sheet boundary layer, *J. Geophys. Res.*, *107*(A8), 1201, doi:10.1029/2001JA900113.

J. Dombeck and J. R. Wygant, School of Physics and Astronomy, University of Minnesota, 116 Church Street SE, Minneapolis, MN 55455, USA.

A. Keiling, F. S. Mozer, and G. K. Parks, Space Sciences Laboratory, University of California, Berkeley, 7 Gauss Way, Berkeley, CA 94720, USA. (keiling@ssl.berkeley.edu)

W. Lotko and A. V. Streltsov, Thayer School of Engineering, Dartmouth College, 8000 Cummings Hall, Hanover, NH 03755, USA.

C. T. Russell, Institute of Geophysics, University of California, Los Angeles, 405 Hilgard Avenue, Los Angeles, CA 90095, USA.